

The effect of finite detection efficiency on the observation of dipole-dipole interaction of a few Rydberg atoms

I. I. Ryabtsev, D. B. Tretyakov, I. I. Beterov, and V. M. Entin

Institute of Semiconductor Physics

Prospekt Lavrentyeva 13, 630090 Novosibirsk, Russia

(Dated: January 22, 2007)

We have developed a simple analytical model describing the multi-atom signals measured in the experiments on dipole-dipole interaction at resonant collisions of a few Rydberg atoms. It has been shown that the finite efficiency of the selective field-ionization detector leads to the mixing up of the spectra of resonant collisions registered for various numbers of Rydberg atoms. The formulae are presented, which help to estimate an appropriate mean Rydberg atom number for a given detection efficiency. We have found that a measurement of the relationship of the amplitudes of collisional resonances observed in the one- and two-atom signals provides a straightforward determination of the absolute detection efficiency and mean Rydberg atom number. We also performed a testing experiment on resonant collisions in a small excitation volume of a sodium atomic beam. The resonances observed for 1 to 4 Rydberg atoms have been analyzed and compared with the theory.

PACS numbers: 34.10.+x, 34.60.+z, 32.80.Rm, 32.70.Jz, 03.67.Lx

I. INTRODUCTION

Experimental and theoretical studies of long-range interactions of highly excited Rydberg atoms are important for the development of quantum information processing with neutral atoms [1]. Strong dipole-dipole (DD) or van der Waals interactions between Rydberg atoms allow for entangling neutral atoms and implementing quantum logic gates [2-7].

Practical realization of the proposed schemes of quantum information processing requires the precise measurements of the number of Rydberg atoms and of their population distribution over Rydberg states. For example, some schemes of two-qubit operations are based on DD interaction of two neighboring atoms, which are shortly excited to Rydberg states [2-6]. After this interaction the composite wavefunction of the two atoms obtains a phase shift that is used to perform a conditional quantum phase gate. To implement such a scheme one needs to measure the population distributions of the two atoms and tune the interaction time to adjust the phase shift to be π . Another example is the dipole blockade effect, which should appear as laser excitation of only one Rydberg atom out of many DD-interacting atoms in a large ensemble due to the interaction-induced changes in the spectra of collective excitations [3,7]. In this case a single Rydberg atom must be unambiguously detected.

The most sensitive detection of Rydberg atoms is achieved with the selective field ionization (SFI) technique that in addition allows for measurements of the population distribution [8]. A typical timing diagram of the SFI detection is shown in Fig. 1(a). A ramp of electric field is applied after each laser excitation pulse at some delay to that defines the time of free Rydberg-Rydberg in-

teraction. Rydberg atoms ionize with almost 100% probability as soon as the electric field reaches a critical value $E_{cr} \approx n^4$, where n is the principal quantum number. Upon ionization, the electrons or ions are detected either by a channeltron or by a microchannel plate (MCP) detector. For the experiments with a few Rydberg atoms the channeltron is preferred since the amplitudes of the channeltron's output pulses are peaked near well-resolved equidistant maxima corresponding to different numbers of detected particles. As an example, in Fig. 1(b) a histogram of the amplitudes of output pulses of the channeltron VEU-6 (GRAN, Russia) used in our experiments is presented. It exhibits the distinct maxima corresponding to 1-5 electrons from the sodium Rydberg atoms detected by SFI after the excitation by pulsed lasers (the mean number of atoms detected per laser pulse in this histogram is about 2.2).

The detection efficiency of channeltrons may reach 90% [9]. However, the actual detection efficiency may be substantially less due to several factors. Firstly, the SFI detection of Rydberg atoms requires the electric field to be homogeneous in order to provide good timing resolution and to distinguish between neighboring Rydberg states. This is achieved by forming the electric field inside a plane condenser. One of its plates should have a hole covered by a metallic mesh to extract charged particles to the channeltron input window [see Fig. 4(a) for our experimental arrangement]. The mesh has a finite effective transparency $T = 50-90\%$. Secondly, the detection efficiency depends on the energy and type of charged particles (electron or ion). Thirdly, after being exposed to the atmosphere, the contamination of the channeltron's working surface by various substances (water, oil, dust, etc.) may reduce the secondary emission of the surface and, as a result, may significantly reduce the overall SFI detection probability.

The above factors can negatively affect the signals and spectra detected in experiments on long-range interac-

Electronic address: ryabtsev@isp.nsc.ru

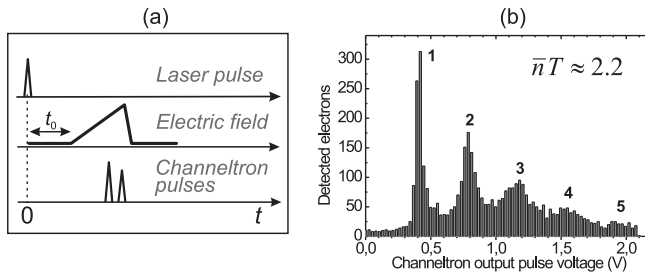


FIG. 1: (a) A typical timing diagram of experiments with selective field ionization (SFI) of Rydberg atoms. (b) The histogram of the amplified output pulses of a channeltron used in our experiments. The observed peaks correspond to 1–5 electrons from the sodium Rydberg atoms detected with SFI after the excitation by pulsed lasers. The mean number of atoms detected per laser pulse $n\bar{T}$ is about 2.2.

tions of a few Rydberg atoms. The main purpose of this article is to analyze theoretically and experimentally the effect of reduced (and actually unknown) detection efficiency on the observed spectra of resonant collisions of a few Rydberg atoms in the electric field. Such collisions lie at the heart of the dipole-blockade effect and other related schemes of quantum information processing. They were investigated in numerous experiments [10–24], but the detection statistics at resonance collisions of a few Rydberg atoms was not studied yet (although recently a sub-Poissonian statistics of the MCP signals at the laser excitation of about 30 Rydberg atoms was studied both experimentally [25] and theoretically [26,27]). We have also implemented a novel method of determining the absolute values of the detection efficiency and mean Rydberg atom number excited per laser pulse. These issues are important for the further development of quantum information processing with Rydberg atoms.

II. LASER EXCITATION AND DETECTION STATISTICS FOR RYDBERG ATOMS

Having N_0 ground-state atoms in the laser excitation volume and probability of excitation of one atom p \approx 1, the mean number of Rydberg atoms excited per laser pulse is

$$n = pN_0 \quad (1)$$

The statistics of the number of Rydberg atoms detected after each laser shot depends on p . In the case of weak excitation (for example, by pulsed broadband laser radiation that is often used in experiments) one has $p \ll 1$, so that Poisson distribution for the probability P_N^{weak} to detect N Rydberg atoms after a single laser shot is applicable:

$$P_N^{\text{weak}} = \frac{(n\bar{T})^N}{N!} e^{-n\bar{T}} \quad (2)$$

In the case of strong excitation (for example, for coherent excitation of Rydberg atoms by narrow band lasers [28,29]) the normal distribution should be used

$$P_N^{\text{strong}} = p^N (1 - p)^{N_0 - N} \frac{N_0!}{N! (N_0 - N)!} \quad (3)$$

which is valid for any p and N_0 . It provides general solutions for the measured signals from Rydberg atoms, although analytical formulae obtained with Eq.(3) are rather complicated. The Poisson distribution is obtained from the normal distribution in the weak excitation limit.

In the further analysis we will ignore a possible effect of the dipole blockade on the above distributions, which was discussed in [25,26], i.e., Rydberg-Rydberg interactions during exciting laser pulses will be neglected. This is the case for appropriately short laser pulses. In this approximation, the above probability distributions would be observed only with an ideal SFI detector of Rydberg atoms. However, for a real detector with the detection efficiency (or effective transmission of the mesh) T these distributions change to

$$P_N^{\text{weak}} = \frac{(n\bar{T})^N}{N!} e^{-n\bar{T}} \quad (4)$$

$$P_N^{\text{strong}} = (pT)^N (1 - pT)^{N_0 - N} \frac{N_0!}{N! (N_0 - N)!} \quad (5)$$

The mean number of Rydberg atoms detected per laser shot thus reduces to nT . For example, the histogram in Fig.1(b) was recorded at $nT = 2.2$, which value has been determined from the measured relationship of the integrated single-atom and two-atom peaks: $P_2^{\text{weak}} = P_1^{\text{weak}} = nT = 2$. The relationships between the other integrated multi-atom peaks are also well described by Eq.(4) at $nT = 2.2$, confirming that the Poisson statistics is valid for the channeltron signals.

Thus, when studying the interactions of a few Rydberg atoms and detecting the atoms by SFI, one should keep in mind that the pure interaction of two Rydberg atoms cannot be observed with non-ideal SFI detectors, since measured two-atom signals would have a contribution from the larger Rydberg atom numbers. This is also true for the possible observations of the dipole blockade. Our aim is to analyze what detection efficiency is tolerable for experiments of such kind.

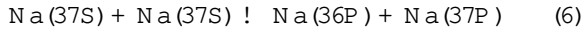
As the number of Rydberg atoms excited in each laser shot is unknown and fluctuates around n , a post-selection technique should be used in order to accumulate the signals for a definite number N of Rydberg atoms detected per laser pulse. In this technique the signals are first

accumulated over many laser pulses. Then the signals are sorted by the atom number (up to 5 atoms in our experiments) according to the measured in advance histogram of the channeltron output pulses [Fig.1(b)]. After this procedure the signals are separately determined for different numbers N of detected Rydberg atoms. This technique has already been demonstrated in our previous experiment on microwave spectroscopy of multi-atom excitations [5].

III. RESONANT COLLISIONS

The DD interaction of Rydberg atoms appears most prominently in the resonant collision processes (also called Forster resonances), which have huge collision cross-sections [8]. A population transfer between Rydberg states induced by such processes can be used as a sensitive probe of DD interaction. In spite of numerous publications on resonant collisions observed in atomic beams [10-13] and cold atom clouds [14-24], the works devoted to the statistics of SFI measurements of resonant collisions at small Rydberg atom numbers were lacking.

In the present work we have analyzed the Rydberg atom statistics and effect of finite detection efficiency on the observed spectra of resonant collisions of a few sodium Rydberg atoms in the electric field, both theoretically and experimentally. A particular collisional resonance under study was the population transfer in the binary collisions:



where $Na(nL)$ stands for a sodium Rydberg atom in highly-excited nL state. Processes of this kind were observed in many alkali atoms and for various resonances. In the case of sodium, the energy resonance arises when the $37S$ state lies midway between the $36P$ and $37P$ states. The resonance is tuned by the Stark effect in the electric field 6.3-7.2 V/cm [Fig.2(a)], depending on the fine-structure components of P -states. It appears as narrow peaks in the dependence of population of the $37P$ state on the electric field after initial excitation of atoms in the $37S$ state. An example of collisional resonances observed in our experiment with velocity-selected atomic beam is shown in Fig.2(b) for the case of one Rydberg atom detected with the post-selection technique. Vertical lines indicate the positions of resonances obtained from a numerically calculated Stark map of the relevant Rydberg states. The other details of the experimental spectrum will be discussed in Sec.VI. We note that the $37P$ sodium atoms are separately detected by SFI, while the $37S$ and $36P$ atoms have almost identical critical electric field for SFI and cannot be individually detected.

Although Eq.(6) is written for binary collisions of two Rydberg atoms, which are associated with collisions in thermal atomic beams [10,11], the many-body phenomena may become important at long interaction times in

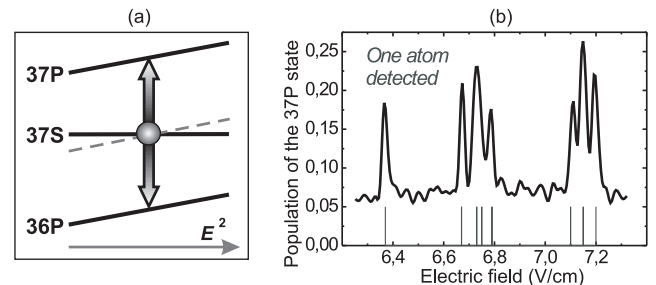


FIG. 2: (a) Sodium energy levels for the resonant collisions $Na(37S) + Na(37S) \rightarrow Na(36P) + Na(37P)$ tuned by the electric field E . (b) An example of the experimental spectrum of collisional resonances in the velocity-selected atomic beam for the case of one sodium Rydberg atom detected. Vertical lines indicate the calculated positions of resonances for various fine-structure components of P -states.

the velocity-selected atomic beams [12,13] and cold atom clouds [14-24]. Therefore, many-body interactions of Rydberg atoms should be considered for the entire ensemble of atoms in the interaction volume.

The nonresonant background processes that can also populate the $37P$ state should be taken into account for the full signal analysis. These are transitions induced by the ambient 300 K blackbody radiation (BBR) [8] and by nonresonant collisions. They give a constant background signal seen in Fig.2(b), which is independent of the Rydberg atom number and electric field.

As discussed above, the SFI technique provides an opportunity of post-selection of the number of Rydberg atoms and their population distribution after each laser pulse. Therefore we can independently measure the resonant collision signals for various numbers N of detected Rydberg atoms by accumulating the statistics for many laser pulses and by their post-selecting. The normalized N -atom signals measured in our experiments are

$$S_N = \frac{n_N(37P)}{n_N(37S) + n_N(36P) + n_N(37P)} \quad (7)$$

where $n_N(nL)$ is the total number of nL Rydberg atoms detected by SFI during the accumulation time for the particular case of N detected Rydberg atoms. An example of the experimentally measured signals S_1 is shown in Fig.2(b).

For an ideal SFI detector Eq.(7) simply gives the population n_N (normalized to 1) of the $37P$ state in a Rydberg atom after having interacted with $(N-1)$ surrounding Rydberg atoms. The approximate formulae for n_N will be obtained in Sec.V for DD interaction in the frozen Rydberg gas and atomic beam. For non-ideal detector various n_N contribute to S_N in a degree that depends on the detection efficiency T and mean Rydberg atom number n , as it will be shown below.

IV. MULTIACTION SIGNALS AT THE FINITE DETECTION EFFICIENCY

The expressions describing n_N (nL) can be explicitly written for any N :

$$\begin{aligned} n_N (37P) &= \sum_{i=N}^8 P_i \frac{i!}{N!(i-N)!} \\ n_N (37S) + n_N (36P) &= \sum_{i=N}^8 P_i \frac{i!}{N!(i-N)!} \end{aligned} \quad (8)$$

where Z is the total number of exciting laser pulses during the accumulation time and P_i is the probability distribution given either by Eq.(2) or Eq.(3). Each term in the above sums represents a contribution from i actually excited Rydberg atoms, and it takes into account its statistical weight and finite detection probability. Each P_i should be viewed as a collision resonance contour in the electric field scale, which would be observed for the interaction of i Rydberg atoms. The radiation damping of Rydberg states is neglected here, i.e., the interaction time is taken to be much shorter than their effective lifetimes of 30 s (37S state) and 70 s (36P and 37P states) at the 300 K ambient temperature.

Taking into account that

$$n_N (37P) + n_N (37S) + n_N (36P) = Z P_N \quad (9)$$

where P_N is the probability distribution given either by Eq.(4) or Eq.(5), the measured, post-selected and averaged over many laser pulses signals of resonant collisions are

$$S_N^{\text{weak}} = e^{n(1-T)} \sum_{i=N}^8 \frac{[n(1-T)]^i}{i!(i-N)!} \quad (10)$$

$$S_N^{\text{strong}} = \frac{(N_0 - N)!}{(N_0 - nT)^{N_0 - N}} \sum_{i=N}^{N_0} \frac{[n(1-T)]^i}{(N_0 - i)!(i - N)!} \quad (11)$$

For an ideal detector ($T = 1$) one obtains the expected identity $S_N = n$ for both distributions, since only $i = N$ term in the sums is nonzero.

One should note that the spectrum of S_N can not have a collision resonance feature since this is a pure single-atom spectrum. The population transfer in S_N may appear only due to the mentioned above background processes from BBR and nonresonant collisions. At the same time, the other spectra (i.e., $n > 1$) should have a constant nonresonant part identical to S_N (as it is independent of the

electric field) and a resonant part S_N^{res} from the Rydberg-Rydberg interactions:

$$n > 1 = S_N + S_N^{\text{res}} \quad (12)$$

The substitution of Eq.(12) into Eq.(10), Eq.(11) and their reduction yield

$$S_N^{\text{weak}} = S_N + e^{n(1-T)} \sum_{i=N}^8 \frac{[n(1-T)]^i}{i!(i-N)!} \quad (13)$$

$$\begin{aligned} S_N^{\text{strong}} &= S_N + \frac{(N_0 - N)!}{(N_0 - nT)^{N_0 - N}} \\ &\quad \sum_{i=N}^{N_0} \frac{[n(1-T)]^i}{(N_0 - i)!(i - N)!} \quad (14) \end{aligned}$$

Therefore, in order to compare the observed amplitudes of collisional resonances, the non-resonant background S_N should be subtracted from these signals. Now it is clear that, as soon as $T < 1$, the resonance features are observable even in the S_N signal, which corresponds to the case of detection of single Rydberg atom. This might be a problem for the attempts to observe the dipole blockade effect, where the detection of single Rydberg atom out of many interacting atoms is required. Eq.(13) and Eq.(14) help to estimate the detection error and the contribution from the higher numbers of actually excited Rydberg atoms. More conclusions will be drawn after evaluating the dependences of S_N^{res} on N in the next section.

V. EVALUATION OF THE MULTIACTION SPECTRA OF RESONANT COLLISIONS

Accurate calculation of S_N^{res} is a challenging problem. It requires to account for any-body interactions [30,31], orientation of atom dipoles [18,21,32], time evolution of dipoles and populations [23,27,31], spatial distribution of Rydberg atoms [18,21,33], coherent and pumping effects at the laser excitation [20,28,29], etc. The sophisticated theoretical models for the spectra of resonant collisions were developed in [30,31]. We will simplify this problem by introducing an average energy of DD interaction between any pair of Rydberg atoms in the atomic ensemble. This corresponds to the spatial and orientational averaging of laser excitation and of Rydberg dipoles over the ensemble. Such approximation is reasonable for our consideration, since we study the signals averaged over many laser excitation and detection events in a disordered atomic ensemble.

We will assume that an ensemble of N_0 sodium atoms in the 3S ground state has a finite volume formed at the point of intersection of the atomic beam or cold atom cloud with exciting laser beam.

The energy levels of sodium atom s relevant to the problem of resonant collisions are $\beta Si = \beta i$, $\beta 6P = \beta i$, $\beta 7Si = \beta i$, and $\beta 7P = \beta i$ [they are shown in Fig.2(a) except the 3S ground state]. These are the states that might be used to observe the dipole blockade effect or two-atom interactions. Other states are not populated by laser excitation or by DD interaction and can be safely ignored in the further analysis. The composite wavefunction of the ensemble can be taken as

$$\Psi_0(t) = \sum_{k=1}^X (C_{0k} \beta i_k + C_{1k} \beta i_k + C_{2k} \beta i_k + C_{3k} \beta i_k) \quad (15)$$

where C_{ik} are time-dependent coefficients for the k^{th} atom in the ensemble. Each atom is thus supposed to be in a coherent superposition state. An initial condition is that immediately after laser excitation ($t = 0$) only C_{0k} and C_{2k} are nonzero. Afterwards the coefficients C_{1k} , C_{2k} and C_{3k} may evolve in time due to DD interaction, while C_{0k} remains unchanged. The Hamiltonian of the ensemble is

$$\hat{H} = \sum_{k=1}^X \hat{H}_k + \hat{V}_{nm} \quad (16)$$

where \hat{H}_k is the unperturbed Hamiltonian of the k^{th} atom, and \hat{V}_{nm} is the operator of binary DD interaction of the n^{th} and m^{th} atom s:

$$\hat{V}_{nm} = \frac{1}{4} \frac{\hat{d}_n \hat{d}_m}{R_{nm}^3} \quad (17)$$

Here \hat{d}_n and \hat{d}_m are dipole moment operators of the n^{th} and m^{th} atom s, R_{nm} is a vector connecting these two atom s, and ϵ_0 is the dielectric constant.

Our aim is to calculate the time evolution of Ψ_0 for a given number N of actually excited Rydberg atom s. In order to do that, we have to decompose the wavefunction of Eq.(15) to a set of the collective states corresponding to different Rydberg atom numbers and then proceed the calculations for certain N . As C_{0k} are not affected by DD interaction, we can simplify the calculations by considering only those parts of the wavefunction, which are related to Rydberg states. These parts are

$$\Psi_N(t) = \sum_{n \neq m}^X A \beta i_1 \beta i_2 \dots \beta i_n \dots \beta i_m \dots \beta i_N + a_{nm} \beta i_1 \beta i_2 \dots \beta i_n \dots \beta i_m \dots \beta i_N \quad (18)$$

where A and a_{nm} are the new coefficients for the collective states of the decomposed wavefunction. These states

are nearly degenerate in energy and therefore experience strong DD interaction, while interactions with the other collective states can be neglected. The sum in Eq.(18) accounts for all possible binary interactions and contains $N(N-1)$ terms.

Solving the Schrodinger equation with Eq.(16)-Eq.(18) in the resonance approximation yields for the time evolution of these coefficients:

$$A = \sum_{n \neq m}^X a_{nm} e^{i \omega t} \quad (19)$$

$$a_{nm} = \frac{i \omega t}{\sum_{n \neq m}^X i \omega n_j a_{nj} + \sum_{j \neq n, m}^{\infty} i \omega j_m a_{jm}} \quad (20)$$

Here $\omega = (2E_{37S} - E_{36P} - E_{37P})/\hbar$ is the detuning from the exact double resonance $36P - 37S - 37P$, which is determined by the Stark-tuned energies E_{nL} of Rydberg states shown in Fig.2(a). The value $\omega_{nm} = \hat{V}_{nm}$ is the energy of the resonant DD interaction $N a(37S) + N a(37S) \rightarrow N a(36P) + N a(37P)$ between n^{th} and m^{th} atom s, which is proportional to the product of dipole moments $d_1 = 36P \hat{d} 37S$ and $d_2 = 37P \hat{d} 37S$. The value $\omega_{nj} = \hat{V}_{nj}$ is the energy of the nonresonant DD interaction $N a(37S) + N a(36P) \rightarrow N a(36P) + N a(37S)$, which is proportional to βi_1^2 . The value ω_{nj}^{∞} is the energy of another nonresonant DD interaction $N a(37S) + N a(37P) \rightarrow N a(37P) + N a(37S)$, which is proportional to βi_2^2 . The two latter interactions are independent of ω and become important as soon as P-states are noticeably populated by the resonant interaction. They have been supposed to be responsible for the decoherence and broadening of collisional resonances in a frozen Rydberg gas [16].

The initial conditions to Eq.(19), Eq.(20), at $t = 0$ may be taken as $a_{nm}(0) = 0$ and $A(0) = \frac{1}{N}$. The latter is chosen from the fact that a measurement of the Rydberg atom number with an ideal detector must give N . After calculating the time dependences of A and a_{nm} , the desired spectra Ψ_N^{res} can be found as

$$\Psi_N^{\text{res}} = \frac{1}{2N} \sum_{n \neq m}^X \beta i_n \beta i_m \quad (21)$$

The factor 1/2 appears because in the resonant collision process an atom in the initial 37S state undergoes the transitions to the 36P and 37P states with equal probabilities, while the sum in Eq.(20) only gives a probability to leave the 37S state. Therefore, the main problem is the calculation of a_{nm} for the particular experimental conditions. We will consider the two most common cases: a frozen Rydberg gas and an atomic beam, which differ in the time dependence of the interaction energy.

A. Frozen Rydberg gas

In a frozen Rydberg gas [14,15] the atoms are almost immobile during the free interaction time [t_0 in Fig.1(a)] of a few microseconds [23]. In this case a_{nm} are constants, and Eq.(19), Eq.(20) are reduced to

$$A_i A + A \sum_{n \neq m} \frac{X}{j_{nm}^2} + e^{i \omega t} \sum_{n \neq m} \frac{X}{j_{nm}^2} \sum_{n \neq m} a_{nj} + \sum_{j \neq n, m} a_{jm} = 0 \quad (22)$$

This equation can only be solved numerically. However, if the last term corresponding the nonresonant interactions in Eq.(22) were absent, this equation would be readily solved with the above initial conditions. The line shape of the resonance for N Rydberg atoms calculated with Eq.(19)–Eq.(22) would exhibit the Rabi-like oscillations:

$$N_{res}(t_0) = \frac{1}{2} \frac{P}{P - \sum_{n \neq m} \frac{j_{nm}^2}{j_{nm}^2 + 4} = 1} \frac{\sin^2 \theta(t_0)}{\sum_{n \neq m} \frac{j_{nm}^2}{j_{nm}^2 + 4} = 4A} \quad (23)$$

This formula is valid at $N_{res}(t_0) = 1/2$, i.e., when the 3P state is weakly populated and the effect of nonresonant interactions in Eq.(22) can be neglected. Indeed, the numerical simulations performed for the interactions of six Rydberg atoms in ref. [23] have shown that nonresonant interactions do not give a noticeable contribution at all. Nevertheless, one should keep in mind that if the population transfer is substantial, the width of the resonance increases and coherent oscillations of Eq.(23) will be washed out [16,23].

The Rabi oscillations in $N_{res}(t_0)$ should disappear due to yet another reason. We note that Eq.(23) is obtained for a single laser shot, which has excited N Rydberg atoms with their specific a_{nm} values. A atom excited by another laser shot would commonly have different a_{nm} values, so that the opposing phase and resonance width in Eq.(23) would also be different. As the signals are accumulated from many laser shots, the spectrum of Eq.(23) is averaged over possible values of the sum it contains. The resonance lineshape thus turns to the Lorentz prefactor of Eq.(23) with the maximum amplitude of $1/4$ [the squared sinus in Eq.(23) is to be replaced with its average value $1/2$].

For the further analysis we need to find a scaling dependence of $N_{res}(t_0)$ on N , at least in the limit of weak DD interaction. We note that the sum it appeared in Eq.(23) have $N(N-1)$ terms and therefore can be represented as

$$\sum_{n \neq m} \frac{1}{j_{nm}^2} = N(N-1)^2 \quad (24)$$

with \sim being the mean energy of resonant DD interaction between any pair of atoms in the ensemble. The averaging should be made over all possible positions of 2 Rydberg atoms among (N_0-2) ground-state atoms in the laser excitation volume. This is a key point of our model, since introducing of allows us to obtain the scaling dependences of the desired signals on N . Note that Eq.(24) has a general form that gives a correct result even at $N=1$, when DD interaction must be absent. It is also important that Eq.(24) is independent of the signs of particular a_{nm} , therefore the averaging should be made for their squared values.

In order to find \sim , we will consider the DD interaction between two arbitrary Rydberg atoms in the laser excitation volume V containing N_0-1 ground-state atoms. A peculiarity of this problem is that after the laser pulse any atom in the excitation volume can be found in a Rydberg state, and that the distant Rydberg atoms may give a contribution comparable to that from the neighboring atoms and cannot be ignored [15,30].

The number density n_0 of ground-state atoms defines the average spacing $R_0 = (4n_0)^{1/3}$ between two neighboring atoms. The angle-averaged energy of DD interaction of two Rydberg atoms spaced by R_0 is estimated from Eq.(17) as

$$\sim = \frac{d_1 d_2}{4 \pi R_0^3} \quad (25)$$

Our aim is to express \sim through n_0 and N_0 . In the averaging procedure for \sim we will use the below qualitative argumentation that seems to be valid for disordered atom ensembles at $N_0 \ll N$.

Let the excitation volume has a spherical shape of radius $R = R_0$, so that the volume is $V = 4\pi R^3/3$. We have to find a mean-square energy of DD interaction of an atom, situated deeply in this volume, with the surrounding $(N_0-1) - N_0$ atoms. The mean atom number in the volume of radius R_0 is $4\pi R_0^3 n_0/3 = 1$. This implies that there are no other atoms at the distances $r < R_0$ from this central atom. Therefore, one should only account for the interaction of this atom with the other atoms situated at $r = R_0$. The mean number of atoms at the distances lying in the interval from r to $r+dr$ is $n_0 4\pi r^2 dr$. Hence, the statistical weight of this spherical layer is $n_0 4\pi r^2 dr = N_0$. Then the averaging is done with an integral

$$\sim = \frac{n_0}{N_0} \int_{R_0}^{\infty} \frac{2R_0^6}{r^6} 4\pi r^2 dr = \frac{\frac{2}{3}R_0^6}{N_0} \quad (26)$$

The relations $N_0 = n_0 V$ and $R = R_0$ have been applied here. The physical meaning of Eq.(26) is that the main contribution to $\langle \cos^2 \theta \rangle$ comes from the nearest-neighbor atom at $r = R_0$, which can be found in a Rydberg state with the $1=N_0$ probability. Although Eq.(26) gives only a rough estimate for the mean-square energy of DD interaction of two arbitrary Rydberg atoms in large disordered atom ensembles, it can be used in the approximate analytical calculations instead of more precise but complicated numerical simulations that must account for the actual geometry of the excitation volume.

Finally, substituting Eq.(24) to Eq.(23), one finds that the full width at half maximum (FWHM) of the collisional resonance at the long interaction time scales as $4 \sqrt{N(N-1)}$. The amplitude of the resonance can be scaled correctly only at the short interaction time or small :

$$a_N^{\text{res}}(t_0; \gamma = 0) = \frac{N(N-1)}{2} t_0^2 \quad (27)$$

The above dependences on N have never been observed for low Rydberg atom numbers, but they are consistent with the results of the earlier theoretical studies of resonant collisions obtained for $N = 1$ [30,31].

B. Atom beam

The atoms in thermal atomic beams have a wide velocity spread (on the order of $v_0 = \sqrt{2k_B T/M} = 680 \text{ m/s}$ at the $T = 650 \text{ K}$ temperature for Na, where k_B is the Boltzmann constant and M is the atom mass). Therefore, the energy of DD interaction of a pair of Rydberg atoms is most likely a rapidly varying function of time [10-13]:

$$a_{nm}(t) = \frac{R_0^3}{v_{nm}^2(t - t_{nm})^2 + b_{nm}^2} \quad (28)$$

Here v_{nm} is the relative velocity of the two atoms, b_{nm} is the impact parameter of collision, and t_{nm} is the time moment when the interaction energy reaches its maximum. In the case of atomic beam both the energy and time of interaction depend on the initial distance R_{nm} between the two Rydberg atoms.

The expected effective interaction time of a few nanoseconds is much shorter than the typical measurement time t_0 of a few microseconds. The population transfer in this case is small, so that Eq.(19) can be solved using the perturbation theory with the conditions $A(t) \text{ const} = N$ and $a_{nm}(t) \ll N$:

$$a_{nm}(t_0) = \frac{p}{iN} \int_0^{Z_0} a_{nm}(t) e^{i\omega t} dt \quad (29)$$

At $v_{nm} \ll (b_{nm} = t_0)$ each pair of Rydberg atoms interact mainly and only one time. If the laser excitation volume is small, then on the average Eq.(28) has its maximum at $t_{nm} = 0$ and falls down to a zero at $t = t_0$. Therefore, t_{nm} in Eq.(28) may be set to 0 and the integration limit in Eq.(29) may be replaced with 0 to t_0 . Then the solution to Eq.(29) is

$$a_{nm}(t_0) = \frac{p}{iN} \frac{R_0^3}{b_{nm} v_{nm}^2} K_1 \left(\frac{b_{nm}}{v_{nm}} \right) \quad (30)$$

where $K_1(x)$ is the modified Bessel function of the second kind. At $|x| < 2$ it has a property that $x K_1(x) = 1 + 2x^2$. Therefore, to some precision, the collision line shape is given by the sum of the Lorentz profiles corresponding to all pairs of Rydberg atoms:

$$N_{\text{res}}^{\text{res}}(t_0) = \frac{1}{2} \frac{2^2 R_0^6}{b_{nm}^4} \frac{X}{[v_{nm}^2 + 2b_{nm}^2]^2} \quad (31)$$

The next step is the averaging of Eq.(31) over v_{nm} and b_{nm} . The main difficulty in averaging over v_{nm} is that the probability distribution for the relative velocity has its maximum at $v_{nm} = 0$ [34]:

$$P(v_{nm}) = \frac{2.96}{2(v_0^2 + 9v_{nm}^2 = 128)} e^{-v_{nm}^2/v_0^2} \quad (32)$$

while Eq.(31) is not valid near $v_{nm} = 0$ at small t_0 . The averaging over velocity distribution may result in the resonance profile with a cusp shape [13] due to the longer interaction time of atoms with low collision velocities. However, if the velocity spread is wide, the relative contribution of low-velocity collisions is small. Therefore, in the following analysis we will use the Lorentzian profiles of Eq.(31), in which we have substituted the mean-square collision velocity $v_{nm}^2 = v_0^2/2$ obtained with Eq.(32).

Further, for the initial distance R_{nm} between the two Rydberg atoms the mean-square impact parameter is estimated as

$$b_{nm}^2 = (R_{nm} \sin \theta)^2 \frac{1}{2} \sin \theta d = \frac{2}{3} R_{nm}^2 \quad (33)$$

Then the pre-averaged resonance line shape is

$$N_{\text{res}}^{\text{res}}(t_0) = \frac{1}{2} \frac{X}{b_{nm}^4} \frac{4.5^2 R_0^6}{(v_0^2 + 8R_{nm}^2)^2} \quad (34)$$

The final averaging over R_{nm} was performed in the same way as we used in previous subsection for the frozen Rydberg gas, i.e., the interaction of an atom with all surrounding atoms was averaged over the interaction distance r :

$$h_N^{\text{res}}(t_0)i \frac{\frac{N(N-1)}{2}n_0}{N_0} \int_{R_0}^{\infty} \frac{45 \frac{2R_0^6}{v_0^2} 4r^2 dr}{r^4(v_0^2 + 8r^2 - 3)} \quad (35)$$

The $\frac{N(N-1)}{2}$ factor has appeared in Eq.(35) since the sum in Eq.(34) contains this number of terms. An analytical solution to Eq.(35) is

$$h_N^{\text{res}}(t_0)i \frac{\frac{N(N-1)}{2} \frac{2}{N_0} \frac{13.5 R_0^2}{v_0^2}}{r} \frac{1}{r} \frac{R_0}{R} + \frac{8 R_0 j j}{3 v_0} \arctan \frac{8 R_0 j j}{3 v_0} \arctan \frac{8 R_0 j j}{3 v_0} \quad (36)$$

It gives a cusp-shaped resonance with the amplitude (at $R_0 = R$)

$$h_N^{\text{res}}(t_0; = 0)i \frac{\frac{N(N-1)}{2} \frac{2}{N_0} \frac{13.5 R_0^2}{v_0^2}}{N_0} \quad (37)$$

The first fraction Eq.(37) represents the scaling dependence on N , the second fraction corresponds to the mean-square interaction energy of two atoms, which is identical to that of Eq.(25) obtained for the frozen Rydberg gas, and the third fraction is the squared effective interaction time. The FWHM of the cusped resonance is

$$r = \frac{\frac{3}{8} \frac{v_0}{R_0}}{3} \quad (38)$$

This width is independent of N and is defined by the effective collision time, as it must be in atom beams [11].

C. Multi-atom signals at weak DD interaction

The multi-atom signals of Eq.(13) and Eq.(14) can be further reduced using the above results on $\frac{h_N^{\text{res}}}{N}$ for the case of weak DD interaction and small population transfer, which is described by Eq.(27) or Eq.(37). One can notice that explicit N dependences of these equations allow us to represent any $\frac{h_N^{\text{res}}}{N}$ through the two-atom spectrum $\frac{h_2^{\text{res}}}{2}$ as

$$\frac{h_N^{\text{res}}}{N} = \frac{1}{2} N(N-1) \frac{h_2^{\text{res}}}{2} \quad (39)$$

The substitution of Eq.(39) into Eq.(13) and Eq.(14) gives after the sum reduction

$$S_N^{\text{weak}} = h_1 + \frac{h_2^{\text{res}}}{2} N(N-1) + N n (1-T) + \frac{1}{2} \ln(1-T)^2 \quad (40)$$

$$S_N^{\text{strong}} = h_1 + \frac{h_2^{\text{res}}}{2} N(N-1) + N n (1-T) \frac{1}{(1-nT-N_0)^2} + \frac{1}{2} \ln(1-T)^2 \frac{N_0}{N_0(1-nT-N_0)^2} \quad (41)$$

It is seen that Eq.(40) can be obtained from Eq.(41) at $N_0 = \max(1, nT)$. This is a criterion for the validity of the Poisson distribution, which means that the number of all atoms in the excitation volume must be much larger than 1 or than the number of detected Rydberg atoms.

The further analysis of signals will be performed with Eq.(40), which is applicable for the most of experimental conditions. For the correctness of measurements, the resonances in S_1 must be small compared to those in $S_{N>1}$. This is the case if $n(N-1) = 2(1-T)$, i.e., if the mean Rydberg atom number is limited to some maximum allowed value. This value is large if only T is close to 1. This condition is important for the experiments aimed at the reliable observation of dipole blockade, when a single Rydberg atom must be unambiguously detected.

At $N > 1$ the criterion of correct measurements of multi-atom signals changes to $n(N-1) = 2(1-T)$. In this case $S_N = h_1 + \frac{h_2^{\text{res}}}{N}$, so that pure interaction of N Rydberg atoms can be studied even with poor detectors, provided n is sufficiently low. For example, for $N = 2$ and $T = 0.1$ one needs $n = 0.6$. One should note that in this case the necessary accumulation time would be long, since the mean number of atoms detected per laser pulse $nT = 0.06$ is small.

Other interesting observations can be made for the relationships between various multi-atom signals. In particular, the signals S_1 and S_2 are of the major importance for the observations of the two-atom interactions and dipole blockade effect. For the Poisson distribution the relationship of their resonant parts is

$$= \frac{S_1}{S_2} = \frac{n(1-T) + \ln(1-T)^2/2}{1 + 2n(1-T) + \ln(1-T)^2/2} = 2 \quad (42)$$

One can see that at $n(1-T) \ll 1$ it is close to $n(1-T)$. In the intermediate case $n(1-T) \gg 1$ the resonance in S_1 is about two times smaller than in S_2 . However, at $n(1-T) \gg 1$ it approaches 1 and the resonances in S_1 and S_2 become of identical amplitudes and shapes, so that it would be impossible to investigate, e.g., pure two-atom interactions.

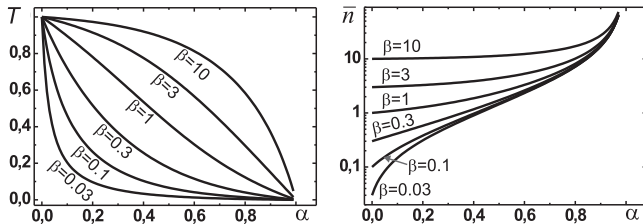


FIG. 3: The calculated dependences of detection efficiency T and mean Rydberg atom number n on the parameters $\beta = (S_1^{\text{weak}} - 1) = (S_2^{\text{weak}} - 1)$ and $\alpha = nT$, which can be measured in experiments.

We have noticed that at the weak laser excitation a measurement of α would allow for a straightforward determination of n ($1 - T$):

$$n(1 - T) = \frac{P}{1 - 2 + 2^2} - \frac{1 + 2}{1} \quad (43)$$

On the other hand, the mean number of Rydberg atoms detected per laser excitation pulse is nT and it can also be readily measured in experiments, e.g., from the histograms like in Fig. 1(b). Therefore, the two above measurements provide an unambiguous determination of the unknown experimental parameters n and T :

$$n = \frac{P}{1 - 2 + 2^2} - \frac{1 + 2}{1} + \quad (44)$$

$$\therefore T = n$$

These formulae are advantageous as they are independent of the specific experimental conditions (atom density, laser intensity, excitation volume, dipole moments, etc.), which are hardly measured, but are necessary to find n and T with conventional methods. In fact, Eq. (44) provides a novel and simple method of the absolute n and T measurements that might be helpful to the further experimental studies on quantum information processing with Rydberg atoms. The calculated dependences of detection efficiency T and mean Rydberg atom number n on the measured parameters α and β are shown in Fig. 3.

V I. EXPERIMENT WITH A SODIUM ATOMIC BEAM

The above theoretical analysis of the Rydberg atom statistics at the SFI detection of resonant collisions needs an experimental confirmation, since no experiments were made earlier for a few Rydberg atoms. We therefore have performed a testing experiment with a sodium atomic beam, in which post-selected signals of resonant collisions were studied for a few detected Rydberg atoms.

A. Experimental setup

An experimental setup was the same as we used in our recent experiments on collisional and BBR ionization of sodium Rydberg atoms [35]. The Na atomic beam with the 650 K temperature ($v_0 = 680 \text{ m/s}$) was formed in a vacuum chamber with the 5×10^{-5} Torr background pressure. The beam was passed between the two stainless-steel plates separated by 10 mm [Fig. 4(a)]. A ramp of pulsed voltage was applied to the upper plate to form a homogeneous electric field for the SFI detection of Rydberg atoms. The lower plate had a 10-mm-diameter hole covered by a mesh with 70% geometrical transparency, through which the electrons appeared in the SFI were guided to an input window of a standard channeltron VEU-6. The laboratory magnetic field was compensated for below 5 mG in all directions by the three pairs of Helmholtz coils. A weak dc electric field was added to the upper plate for the Stark tuning of resonant collisions.

The initial $37S_{1/2}$ Rydberg state was excited via the two-step scheme $3S_{1/2} \rightarrow 3P_{3/2} \rightarrow 37S_{1/2}$. The first step at 589 nm was excited by either pulsed (5 kHz) or cw Rhodamine 6G dye-laser. The broadband pulsed radiation (20 GHz linewidth) could excite the atoms of all velocities, while the narrowband cw radiation (10 MHz linewidth) provided a velocity selection at the cycling hyperfine transition $3S_{1/2}(F=2) \rightarrow 3P_{3/2}(F'=3)$. The second excitation step $3P_{3/2} \rightarrow 37S_{1/2}$ at 410 nm was driven by the second harmonic of a pulsed titanium-sapphire laser having 5 kHz repetition rate, 50 ns pulses, and 10 GHz linewidth.

In order to work with a few strongly interacting Rydberg atoms, we had to localize a small excitation volume, where only closely spaced atoms could be excited. In our experiments we attained this using a crossed-beam geometry shown in Fig. 4(a). The two exciting laser beams were focused to the waists of 50 μm in diameter and intersected at the right angles inside the atomic beam, with both laser beams being at the 45° angles to the atomic beam. We thus formed the excitation volume of about 50 μm size that provided the mean spacing of a few microns between Rydberg atoms. The laser powers were adjusted to detect a few Rydberg atoms per laser pulse on the average.

A timing diagram of signals was identical to that of Fig. 1(a) with the free DD interaction time $t_0 = 3 \text{ s}$. The applied ramp of the electric field stopped this interaction, since the Stark shifts in this field were much larger than the estimated DD interaction energies. The channeltron output pulses from the $37P$ and $(37S + 36P)$ states appeared at the 5 and 5.6 s, correspondingly. They were detected using two independent gates. An integrator and analog-to-digital converter measured their charges after each laser pulse. The channeltron provided the atom-number resolution according to the measured histogram of Fig. 4(b). The amplified single-electron pulses had 400 mV average amplitudes that fluctuated within 350–

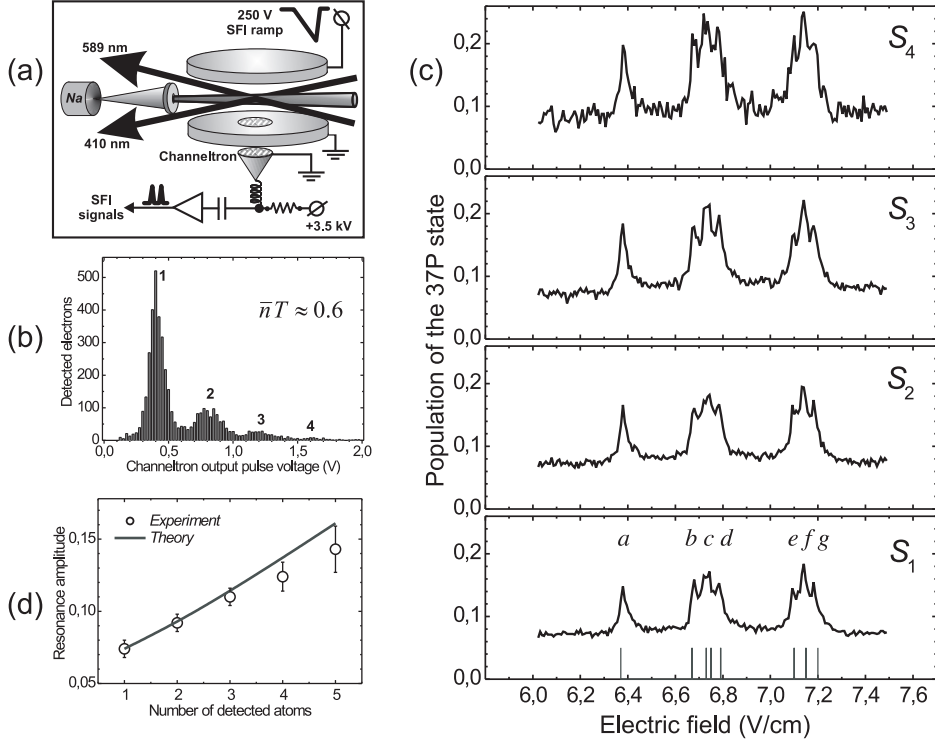


FIG. 4: (a) The arrangement of the experiment on resonant collisions in Na atomic beam. (b) The histogram of the amplified output pulses of a new 32-mm wide channeltron VEU-6 measured at the mean number of atoms detected per laser pulse $\bar{n}T = 0.6$. (c) The experimental spectrum of collisional resonances observed in the Na atomic beam for 1 to 4 Rydberg atoms detected. Vertical lines indicate the calculated positions of resonances for various fine-structure components of P -states. (d) The comparison between experiment and theory for the dependence of the amplitude of resonance a on the number of detected Rydberg atoms.

450 mV from pulse to pulse with almost Gaussian distribution of amplitudes. The two-electron pulses had 800 mV average amplitudes and fluctuated within 700–900 mV. The three-electron pulses were peaked at 1200 mV, and so on. Although the neighboring multi-atom signals in the histograms are overlapping to some extent, the estimated fidelity of the correct N determination is > 90% for the single-atom signal and > 80% for the two-atom signal.

In order to record the spectra, the dc electric field, which controlled the detuning of resonant collisions, was set to the certain values, and for each of them the channeltron signals were accumulated for 10^3 – 10^5 laser pulses. Then the signals were automatically post-selected and sorted by the number of detected Rydberg atoms. After this procedure the experimental signals S_N of Eq.(7) were obtained simultaneously for various N .

B. Experimental results

The experiments on resonant collisions were performed at the volume density $8 \cdot 10^6 \text{ cm}^{-3}$ of ground-state atoms. This value corresponds to the average spacing between neighboring atoms $R_0 = 1.44 \text{ m}$ and to the atom num-

ber $N_0 = 10^4$ in the $V = 50 \text{ m}^3$ excitation volume. At this density the collision resonances were reliably observed in the S_1 signal with both pulsed and cw lasers at the first excitation step. The resonances obtained with cw laser were presented in Fig. 2(b). These were the narrowest resonances observed in our experiments. Unfortunately, the use of cw laser significantly reduced the number of atoms excited to the intermediate $3P_{3/2}$ state due to the velocity selection and partial optical pumping to the $3S_{1/2}$ ($F=1$) ground state, so that detection of resonances in the S_2 – S_4 signals required too long accumulation time. Therefore, the further experiments were performed with the pulsed laser in order to provide an appropriate signal-to-noise ratio in the multi-atom signals, at the cost of somewhat broader resonances.

The multi-atom spectra of resonant collisions S_1 – S_4 observed with the pulsed 589 nm laser are presented in Fig. 4(c). The spectrum for S_5 is not shown since it had significant noise due to low probability of detection of 5 atoms, as can be seen from the histogram of Fig. 4(b). The seven peaks a – g in Fig. 4(c) are due to various transitions to the fine-structure components of P -states (actually, nine peaks should be seen, but peaks c and f have two unresolved components). The positions of the

resonances well coincide with the values obtained from the numerically calculated Stark map of the relevant Rydberg states [see vertical lines in Fig.4(c)].

The shapes of the resonances are cusped at their centers and cannot be properly approximated by a Lorentz profile, in agreement with Eq.(37). We will consider in more detail the double resonance $36P_{J=3=2; M_J, J=1=2} \pm 37S_{J=1=2; M_J, J=1=2} \pm 37P_{J=3=2; M_J, J=1=2}$ that corresponds to the well-resolved single peak a observed at $E = 6.37 \text{ V/cm}$ in the spectrum of resonant collisions in Fig.4(c). Its FWHM is $E = (35 - 3) \text{ mV/cm}$. This width can be converted to the effective frequency width

using the formula obtained in the quadratic Stark effect approximation:

$$= (2 \cdot 37S \cdot 36P \cdot 37P) E \cdot E \quad (45)$$

where n_L are the polarizabilities of n_L Rydberg states measured in our earlier microwave experiments [36]. The polarizability of the $37S$ state is $37S = +3.7 \text{ MHz}/(\text{V/cm})^2$, while the polarizabilities of the above Stark sublevels of P -states are $36P = 104 \text{ MHz}/(\text{V/cm})^2$ and $37P = 127 \text{ MHz}/(\text{V/cm})^2$. One obtains that the FWHM of resonance a is $(53 - 5) \text{ MHz}$. This experimental value well agrees with the theoretical value $= (2 \cdot 46) \text{ MHz}$ calculated from Eq.(38).

As predicted by the theory, the amplitudes of the resonances in Fig.4(c) grow with the increase of the number of detected Rydberg atoms, although we expected this effect to be more pronounced. In order to compare the observed amplitude of resonance a with theory, the radial parts of dipole moments of the $37S - 36P$ and $37S - 37P$ transitions were numerically calculated and found to be 1372 and 1439 a.u., correspondingly. Although these values are valid only for a zero electric field, the mixing of Rydberg states in the field 6.37 V/cm does not significantly alter them, and they may be used for the estimates. The angular parts of both dipole moments are $P_{2=3}^2$. From Eq.(24) and Eq.(25) one obtains $\alpha_0 = (2 \cdot 140) \text{ MHz}$ and $\alpha_1 = (2 \cdot 1.4) \text{ MHz}$. Then Eq.(37) yields the theoretical value $\alpha_2^{\text{res}}(\alpha_0 = 0) = 0.0046$.

Further, at the pulsed laser excitation in the histogram of Fig.4(b) we observed the integral of the two-atom peak (taken over 600–1000 mV) being nearly 3.3 times less than the integral of the single-atom peak (taken over 200–600 mV). Their relationship can be found from Eq.(4) as $P_2^{\text{weak}} = P_1^{\text{weak}} = nT = 2$, hence $\alpha_0 = nT = 0.6$ in our experiment with the pulsed laser. The parameter $\alpha_0 = 0.8$ of Eq.(42) was determined from the observed relationship $(S_{1-1}) = (S_{2-1}) = 0.075 = 0.095$ between the single- and two-atom amplitudes of peak a in Fig.4(c). Finally, Eq.(44) has yielded the unknown experimental parameters $n = 8$ and $T = 8\%$. This means that the resonances observed in Fig.4(c) were not from 1 to 4 Rydberg atoms, but actually from 8 to 30 atoms.

Such a low detection efficiency in the atom-in-beam experiment was quite surprising to us, since we specially

installed a new made channeltron and expected T to be close to the geometrical transparency of the detector mesh (70%). With the old channeltron the detection efficiency was even less, although it provided narrower peaks in the histograms [the histogram in Fig.1(b) was measured with this old channeltron] than the new channeltron in the histogram of Fig.4(b). Our attempts to improve the SFI detection system (usage of a more transparent mesh, acceleration of electrons prior to detection, detection of ions instead of electrons, cleaning of the channeltron's surface, etc.) did not noticeably increase the efficiency. We have concluded that the possible reason could be a rather poor vacuum condition ($5 \cdot 10^{-10} \text{ Torr}$), which could not be proved with the used oil-diffusion pumps required to work with a dense Na beam. Nevertheless, we have demonstrated that the above measurements provide a tool to determine unknown T , which may degrade during the course of any experiments and therefore should be periodically checked out. We may recommend our method to be applied in those experiments with Rydberg atoms where the absolute detection efficiency is crucial.

Finally, with the above experimental values for n , T , and amplitude $S_{1-1} = 0.075$ of peak a, using Eq.(40) we have determined the experimental value $\alpha_2^{\text{res}}(\alpha_0 = 0) = 0.0022 \pm 4$. It satisfactorily agrees with the theoretical value 0.0046, taking into account the approximations adopted in our theoretical model. Furthermore, we can compare the values for the amplitudes of observed resonances to those calculated with Eq.(40) at $\alpha_2^{\text{res}}(\alpha_0 = 0) = 0.0022$. These are shown in Fig.4(d), where we also added an experimental point for S_5 extracted from its noisy spectrum. The experimental and theoretical dependences coincide well for lower N , but start to deviate for higher N . This deviation can be attributed to a saturation of resonances at $N = 4$, as their amplitudes in Fig.4(c) approach to the theoretical limit of $1/4$, while Eq.(40) was derived with the perturbation theory. A comparison between experiment and theory for the other peaks in Fig.4(c) has demonstrated a satisfactory agreement.

The further experimental efforts should be focused on the cold Rydberg atoms. This would help to test our model at the longer interaction times, which are of interest to quantum information processing. The microwave spectroscopy of resonant collisions [37] and long-range interactions [38,39] can be additionally applied as a sensitive probe and control tool.

VII. CONCLUSIONS

The developed theoretical model describes multi-atom signals that could be measured in the experiments on long-range interactions of a few Rydberg atoms. Although several simplifying approximations were used to obtain the analytical formulae, their validity has been partly confirmed by the satisfactory agreement with the

rst experimental data obtained for the resonant collisions of a few Rydberg atoms in the atomic beam. The main result is that finite detection efficiency of the selective field-ionization detector leads to the mixing up of the spectra of resonant collisions associated with various numbers of detected atoms. In particular, the collisional resonance features may appear even in the single-atom signal if the detection efficiency is low. This may impede the possible observations of the dipole blockade or coherent two-atom collisions, which are required to perform quantum gates in quantum information processing schemes. The obtained formulae are helpful in estimating the appropriate mean number of Rydberg atoms excited per laser pulse at a given detection efficiency.

We have shown that the measurement of the relationship between the amplitudes of resonances observed in the single- and two-atom signals provides the straightforward determination of the absolute detection efficiency and mean Rydberg atom number, which are hardly measured by other methods. This novel method is advantageous as it is independent of the specific experimental

conditions (atom density, laser intensity, excitation volume, dipole moments, etc.).

The further experimental tests with a frozen Rydberg gas would be of great interest. In this case the amplitudes of resonances should behave as $N_p^{(N-1)}$, while their width should be proportional to $N(N-1)$. These dependences have never been observed for low Rydberg atom numbers N , since all earlier experiments were made for $N = 1$. The theoretical and experimental results reported in this article might be helpful to the development of quantum information processing with Rydberg atoms.

Acknowledgments

This work was supported by the Russian Foundation for Basic Research, Grant No. 05-02-16181, by the Russian Academy of Sciences, and by INTAS, Grant No. 04-83-3692.

[1] P. S. Jessen, D. L. Haycock, G. K.lose, G. A. Smith, I. H. Dutsch, and G. K. Bremmer, *Quantum Information and Computation* 1, 20 (2001).

[2] D. Jaksch, J. I. Cirac, P. Zoller, S. L. Rolston, R. Cote, and M. D. Lukin, *Phys. Rev. Lett.* 85, 2208 (2000).

[3] M. D. Lukin, M. F. Fleischhauer, R. Cote, L. M. Duan, D. Jaksch, J. I. Cirac, and P. Zoller, *Phys. Rev. Lett.* 87, 037901 (2001).

[4] I. E. Protsenko, G. Reymond, N. Schlosser, and P. Grangier, *Phys. Rev. A* 65, 052301 (2002).

[5] I. I. Rabi, D. B. Trtyakov, and I. I. Beterov, *J. Phys. B* 38, S421 (2005).

[6] M. S. man and T. G. Walker, *Phys. Rev. A* 72, 022347 (2005).

[7] M. S. man and T. G. Walker, *Phys. Rev. A* 72, 042302 (2005).

[8] Rydberg States of Atoms and Molecules, ed. by R. F. Stebbings and F. B. Dunning (Cambridge University Press, Cambridge, 1983); T. F. Gallagher, *Rydberg Atoms* (Cambridge University Press, Cambridge, 1994).

[9] Burle Electro-Optics Inc., <http://www.burle.com/cgi-bin/bytesserver.pl/pdf/ChannelBook.pdf>

[10] K. A. Sanya, J. F. Delpach, F. Gounand, W. Sandner, and T. F. Gallagher, *Phys. Rev. Lett.* 47, 405 (1981).

[11] T. F. Gallagher, K. A. Sanya, F. Gounand, J. F. Delpach, W. Sandner, and R. Kachru, *Phys. Rev. A* 25, 1905 (1982).

[12] R. C. Stoneman, M. D. Adams, and T. F. Gallagher, *Phys. Rev. Lett.* 58, 1324 (1987).

[13] J. R. Veale, W. A. Anderson, M. Gatzke, M. Renn, and T. F. Gallagher, *Phys. Rev. A* 54, 1430 (1996).

[14] W. R. Anderson, J. R. Veale, and T. F. Gallagher, *Phys. Rev. Lett.* 80, 249 (1998).

[15] I. M.ouradko, D. Compart, F. de Tomasi, A. F. Boretti, P. Noosbaum, V. M. Akulin, and P. Pillet, *Phys. Rev. Lett.* 80, 253 (1998).

[16] W. R. Anderson, M. P. Robinson, J. D. D. Martin, and T. F. Gallagher, *Phys. Rev. A* 65, 063404 (2002).

[17] A. L. de Oliveira, M. W. Mancini, V. S. Bagnato, and L. G. M. Arcassa, *Phys. Rev. Lett.* 90, 143002 (2003).

[18] T. J. Carroll, K. Claringbould, A. Goodsell, M. J. Lim, and M. W. Noel, *Phys. Rev. Lett.* 93, 153001 (2004).

[19] I. M.ouradko, Wenhui Li, and T. F. Gallagher, *Phys. Rev. A* 70, 031401(R) (2004).

[20] M. M. udrich, N. Zahzam, T. Vogt, D. Compart, and P. Pillet, *Phys. Rev. Lett.* 95, 233002 (2005).

[21] T. J. Carroll, S. Sunder, and M. W. Noel, *Phys. Rev. A* 73, 032725 (2006).

[22] T. Vogt, M. Viteau, J. Zhao, A. Chotia, D. Compart, and P. Pillet, *Phys. Rev. Lett.* 97, 083003 (2006).

[23] S. W. estermann, T. Amthor, A. L. de Oliveira, J. D. Eigmayer, M. Reetz-Lamour, and M. W. eidem uller, *European Physical Journal D* 40, 37 (2006).

[24] K. A. froushesh, P. Bohlouli-Zanjani, J. A. Petrus, and J. D. D. Martin, *Phys. Rev. A* 74, 062712 (2006).

[25] T. Cubel Liebisch, A. Reinhard, P. R. Berman, and G. Raithel, *Phys. Rev. Lett.* 95, 253002 (2005).

[26] C. Ates, T. Pohl, T. Pattard and J. M. Rost, *J. Phys. B*, 39, L233-L239 (2006).

[27] J. V. Hernandez and F. Robicheaux, *J. Phys. B*, 39, 4883 (2006).

[28] T. Cubel, B. K. Teo, V. S. Malinovsky, J. R. Guest, A. Reinhard, B. Kuman, P. R. Berman, and G. Raithel, *Phys. Rev. A* 72, 023405 (2005).

[29] J. D. Eigmayer, M. Reetz-Lamour, T. Amthor, S. W. estermann, A. L. de Oliveira, and M. W. eidem uller, *Optics Communications* 264, 293 (2006).

[30] V. M. Akulin, F. de Tomasi, I. M.ouradko, P. Pillet, *Physica D* 131, 125 (1999).

[31] J. S. Frasier, V. Celli, and T. Blum, *Phys. Rev. A* 59, 4358 (1999).

[32] T. G. Walker and M. S. man, *J. Phys. B* 38, S309

(2005).

[33] F. Robicheaux, J.V. Hernandez, T. Topcu, and L.D. Nordam, *Phys. Rev. A* **70**, 042703 (2004).

[34] K. Micalis, I. I. Beterov, N. N. Bezuglov, I. I. Ryabtsev, D. B. Trtyakov, A. Ekers, A. N. Klicharev, *J. Phys. B*, **38**, 1811 (2005).

[35] I. I. Beterov, D. B. Trtyakov, I. I. Ryabtsev, N. N. Bezuglov, K. Micalis, A. Ekers, and A. N. Klicharev, *J. Phys. B* **38**, 4349 (2005).

[36] I. I. Ryabtsev and D. B. Trtyakov, *JETP* **94**, 677 (2002).

[37] S. Osnaghi, P. Bertet, A. Alleva, P. M. Ajoli, M. Brune, J. M. Raimond, and S. Haroche, *Phys. Rev. Lett.* **87**, 037902 (2001).

[38] K. A. Froushesh, P. Bohlouli-Zanjani, D. Vagale, A. Mugford, M. Fedorov, and J. D. D. Martin, *Phys. Rev. Lett.* **93**, 233001 (2004).

[39] K. A. Froushesh, P. Bohlouli-Zanjani, J. D. Carter, A. Mugford, and J. D. D. Martin, *Phys. Rev. A* **73**, 063403 (2006).